JOURNAL OF SPACECRAFT AND ROCKETS
Vol. 47, No. 1, January–February 2010

Compressibility Considerations for k-ω Turbulence Models in Hypersonic Boundary-Layer Applications

Christopher L. Rumsey*
NASA Langley Research Center, Hampton, Virginia 23681-2199

DOI: 10.2514/1.45350

The ability of k-ω models to predict compressible turbulent skin friction in hypersonic boundary layers is investigated. Although uncorrected two-equation models can agree well with correlations for hot-wall cases, they tend to perform progressively worse (particularly for cold walls) as the Mach number is increased in the hypersonic regime. Simple algebraic models such as Baldwin–Lomax perform better compared to experiments and correlations in these circumstances. Many of the compressibility corrections described in the literature are summarized here. These include corrections that have only a small influence for k-ω models or that apply only in specific circumstances. The most widely used general corrections were designed for use with jet or mixing-layer free-shear flows. A less-well-known dilatation–dissipation correction intended for boundary-layer flows is also tested and is shown to agree reasonably well with the Baldwin–Lomax model at cold-wall conditions. It exhibits a less dramatic influence than the free-shear type of correction. There is clearly a need for improved understanding and better overall physical modeling for turbulence models applied to hypersonic boundary-layer flows.

Nomenclature

A	=	function in skin-friction correlation, Eq. (A6)
a	=	speed of sound, function in skin-friction correlation, Eq. (A8)
a_1	=	constant in Bradshaw's relation, 0.31
B	=	function in skin-friction correlation, Eq. (A7)
b	=	function in skin-friction correlation, Eq. (A9)
C_f	=	skin-friction coefficient, Eq. (A1)
C_h	=	heat transfer coefficient, Eq. (A15)
C_μ	=	coefficient used in two-equation models, 0.09
c_p	=	specific heat at constant pressure
d	=	distance from the wall
E	=	specific total energy
e	=	specific internal energy
F_c	=	function in skin-friction correlation, Eq. (A4)
F_{Re_θ}	=	function in skin-friction correlation, Eqs. (A10–A12)
F_1	=	shear-stress transport blending function
$\mathcal{H}$	=	Heaviside function
h	=	enthalpy
k	=	turbulent kinetic energy, thermal conductivity coefficient
ℓ	=	length scale
M	=	Mach number, U_∞/a_∞
M_T	=	turbulence Mach number, $\sqrt{2k}/a$
M_{T_0}	=	constant for dilatation–dissipation correction
$\mathcal{P}$	=	turbulence production term, Eq. (3)
Pr_t	=	turbulent Prandtl number
p	=	pressure
q	=	heat flow, $-k\nabla T$
q_T	=	turbulent heat-flux vector in the Favre-averaged energy equation
R_{af}	=	Reynolds analogy factor
Re	=	Reynolds number, $\rho_\infty U_\infty \ell/\mu_\infty$
Re_x	=	Reynolds number based on x distance, $\rho_\infty U_\infty x/\mu_\infty$
Re_θ	=	Reynolds number based on momentum thickness, $\rho_\infty U_\infty \theta/\mu_\infty$
r	=	recovery factor
S'	=	constant in Sutherland's law
S_{ij}	=	strain rate tensor, Eq. (5)
$\bar{S}_{ij}$	=	traceless strain rate tensor, Eq. (23)
St	=	Stanton number, Eq. (A15)
T	=	temperature
t	=	time
T_0	=	constant in Sutherland's law
Tu	=	turbulence intensity, Eq. (9)
U	=	velocity
u_j	=	velocity component
$\overline{u_i' u_j'}$	=	fluctuating velocity correlation
W_{ij}	=	rotation rate tensor, $\frac{1}{2}(\partial u_i/\partial x_j - \partial u_j/\partial x_i)$
x_j	=	Cartesian coordinate
y	=	distance from the wall
y^+	=	distance from the wall in inner-law variables, $\sqrt{(\rho\tau_w)}y/\mu$
α	=	coefficient for two-equation model
α_2, α_3	=	constants in Sarkar's model
β, β^*	=	coefficients for two-equation model
β_c, β_c^*	=	compressibility-corrected coefficients for two-equation model
γ	=	ratio of specific heats
δ_{ij}	=	Kronecker delta
ε	=	turbulent dissipation per unit mass
θ	=	momentum thickness
κ	=	Karman constant, 0.41
Λ	=	constant for dilatation–dissipation correction
μ	=	viscosity
μ_0	=	constant in Sutherland's law
ν	=	kinematic viscosity, μ/ρ
ξ^*	=	constant for dilatation–dissipation correction
ρ	=	density
σ_k, σ_ω, $\sigma_{\omega 2}$	=	coefficients for two-equation model
τ_{ij}	=	turbulent shear stress, Eq. (4)
τ_w	=	wall shear stress, $\mu_w \partial u/\partial y\|_w$
Ω	=	magnitude of vorticity, $\sqrt{2W_{ij}W_{ij}}$
ω	=	dissipation per unit turbulent kinetic energy

Subscripts

aw	=	adiabatic wall

Received 8 May 2009; revision received 10 September 2009; accepted for publication 19 September 2009.

*Senior Research Scientist, Computational Aerosciences Branch, Mail Stop 128. Associate Fellow AIAA.

e	=	edge
ideal	=	ideal
incomp	=	incompressible
inf	=	freestream
std	=	standard
t	=	turbulent
w	=	wall
1	=	first grid cell off the wall
∞	=	freestream

I. Introduction

COMPRESSIBILITY is typically not considered to be important for wall-bounded turbulent flows over a wide range of Mach numbers. As stated in Wilcox [1] (p. 239),

> Generally speaking, compressibility has a relatively small effect on turbulent eddies in wall-bounded flows. This appears to be true for Mach numbers up to about 5 (and perhaps as high as 8), provided the flow does not experience large pressure changes over a short distance such as we might have across a shock wave. At subsonic speeds, compressibility effects on eddies are usually unimportant for boundary layers provided $T_w/T_e < 6$.

The hypothesis of Morkovin [2] states that the compressibility effects on turbulence can be accounted for by mean density variations alone. For many applications, this hypothesis has proved correct in that good results can be obtained for mean velocity and temperature fields using incompressible turbulence models extended directly to compressible turbulent boundary layers. Furthermore, So et al. [3] have shown the Morkovin hypothesis to be equally applicable for prediction of the turbulence field itself, for flat-plate boundary layers up to a Mach number of at least 10. They state, "there is indeed a dynamic similarity of the incompressible and compressible mean and turbulence field, and the Morkovin hypothesis is valid for both fields." In other words, for many subsonic through hypersonic boundary-layer applications, the incompressible forms of turbulence models (with mean density variations accounted for) are expected to be reasonable approximations.

The most common classes of compressibility correction for Reynolds-averaged Navier–Stokes turbulence models were developed for the purpose of improving correlations with experiment for free-shear layer or jet spreading rates (see, for example, [4–6]). However, what we are concerned with here is primarily (attached) hypersonic boundary-layer flow. In this paper, compressibility corrections (particularly applicable to boundary-layer flows) from the literature are described. The focus here is solely on the k-ω form of two-equation models. The claim that compressibility corrections are not required for hypersonic boundary-layer flows is investigated for a wide range of Mach numbers and wall-temperature boundary conditions.

The paper is organized as follows. First, considerations for k-ω models are discussed. Then, compressibility corrections for two-equation models from the literature are summarized. Finally, results for hypersonic boundary-layer flows are shown, and conclusions are made.

II. Considerations for k-ω Models

Two widely used k-ω models are due to Wilcox [1,7] and Menter [8]. The Wilcox model has undergone several changes since 1988; the latest version is referred to here as Wilcox06. The Menter model is the shear-stress transport version, referred to as SST. Full descriptions of these models can be found in their respective references.

For situations in which compressibility is important (and shocks may be present), the turbulence equations are typically solved in conservation form. For example, the SST model is written

$$\frac{\partial(\rho k)}{\partial t} + \frac{\partial(\rho u_j k)}{\partial x_j} = \mathcal{P} - \beta^* \rho \omega k + \frac{\partial}{\partial x_j}\left[(\mu + \sigma_k \mu_t)\frac{\partial k}{\partial x_j}\right] \quad (1)$$

$$\frac{\partial(\rho \omega)}{\partial t} + \frac{\partial(\rho u_j \omega)}{\partial x_j} = \frac{\alpha \rho}{\mu_t}\mathcal{P} - \beta \rho \omega^2 + \frac{\partial}{\partial x_j}\left[(\mu + \sigma_\omega \mu_t)\frac{\partial \omega}{\partial x_j}\right] + 2\rho(1 - F_1)\frac{\sigma_{\omega 2}}{\omega}\frac{\partial k}{\partial x_j}\frac{\partial \omega}{\partial x_j} \quad (2)$$

where

$$\mathcal{P} = -\tau_{ij}\frac{\partial u_i}{\partial x_j} \quad (3)$$

and

$$\tau_{ij} = \rho\overline{u_i' u_j'} = -2\mu_t\left(S_{ij} - \frac{1}{3}\frac{\partial u_k}{\partial x_k}\delta_{ij}\right) + \frac{2}{3}\rho k \delta_{ij} \quad (4)$$

$$S_{ij} = \frac{1}{2}\left(\frac{\partial u_i}{\partial x_j} + \frac{\partial u_j}{\partial x_i}\right) \quad (5)$$

Note that the definition for τ_{ij} varies in the literature: sometimes it is defined with the opposite sign, and sometimes it is defined without the density. The definition does not matter as long as the production term is defined appropriately in Eq. (3), with $+2\mu_t S_{ij}(\partial u_i/\partial x_j)$ as the leading term in $\mathcal{P}$.

It is unclear whether the turbulence model equation form (conservative vs nonconservative) makes much difference in the common situation in which the turbulence models are solved separately (loosely coupled) from the conservative mean flow equations. But certainly if the equations are fully coupled, all should be solved consistently in conservation form.

For flows in which the turbulent kinetic energy is nonnegligible compared to the square of the mean velocity, the k contributes to the conservation of total energy via $\rho E = \rho(e + \frac{1}{2}u_i u_i + k)$ (see Wilcox [1]). Also, the molecular and turbulent diffusion of k, typically modeled as

$$\frac{\partial}{\partial x_j}\left[(\mu + \sigma_k \mu_t)\frac{\partial k}{\partial x_j}\right] \quad (6)$$

in the mean flow energy equation [9], should be included. Furthermore, the perfect gas equation of state then becomes [10]: $p = (\gamma - 1)\rho(E - \frac{1}{2}u_i u_i - k)$. Because many computational fluid dynamics (CFD) codes include other (simpler) turbulence models in addition to two-equation models, for which k is not available, the turbulent kinetic energy contribution to total energy (and its explicit appearance in the energy equation and equation of state) is sometimes ignored.

In an often-used variant of the k-ω model, the production term is simplified by an approximation that makes use of the local magnitude of vorticity Ω:

$$\mathcal{P} = \mu_t \Omega^2 - \frac{2}{3}\rho k \delta_{ij}\frac{\partial u_i}{\partial x_j} = \mu_t \Omega^2 - \frac{2}{3}\rho k \frac{\partial u_k}{\partial x_k} \quad (7)$$

This vorticity source term can be a reasonable approximation of the exact source term in boundary-layer flows [11], and its use can avoid some numerical difficulties sometimes associated with the use of the exact source term. Again, it is common to ignore the $(2/3)\rho k$ term in the production source of Eq. (7) for many applications, but this may have a nonnegligible influence for high-speed flows.

Recommended wall boundary conditions for k-ω models are [8] $k_w = 0$ and $\omega_w = 60\nu/[\beta(\Delta d_1)^2]$. Other boundary conditions for ω are also used, including both smooth and rough walls [1]. The far-field boundary conditions are more difficult to define with confidence. Part of the problem is that the freestream levels are not preserved; they decay rapidly (both due to the equations themselves as well as due to typically coarse grid spacing in the far field). This decay, which occurs for k-ε equations as well, makes the local ambient levels near the body a function of the far-field grid extent. In the freestream, the k-ω governing equations dictate that the decay of eddy viscosity occurs according to

$$\mu_t = \mu_{t,\infty}\left[1 + \beta\omega_\infty \frac{x}{U_\infty}\right]^{1-(0.09/\beta)} \tag{8}$$

where x is the distance from the location where the boundary conditions are set. As discussed in Spalart and Rumsey [12], real flow over external aerodynamic configurations has no reason to obey the decay equations used to calibrate two-equation models in isotropic turbulence. In reality, the kinetic energy (and eddy viscosity) relevant to the aircraft flow varies very little over the size of the typical CFD domain. Thus, the behavior represented by decaying freestream turbulence is not representative of reality. Reference [12] describes the use of sustaining terms that, when added to the k-ω equations, preserve the freestream levels without decay. Although maintaining freestream turbulence is probably important from the point of view of numerical-transition consistency with grid refinement, at high Reynolds numbers the effect is generally small. Therefore, results in this paper will not use the sustaining terms.

For typical subsonic/transonic/supersonic applications, most CFD application codes have developed their own methodology for setting far-field boundary conditions for k and ω, in order to yield reasonable results across a broad range of problems. For example, in CFL3D (Krist et al. [13]), the boundary conditions are $k/a_\infty^2 = 9 \times 10^{-9}$ and $\omega\mu_\infty/(\rho_\infty a_\infty^2) = 1 \times 10^{-6}$, which always gives $\mu_{t,\infty}/\mu_\infty = 0.009$. Because the freestream turbulence level Tu (in percent) is given by

$$\text{Tu}\,,\% = 100\sqrt{\frac{2}{3}\frac{k}{U_\infty^2}} \tag{9}$$

this means that a fixed $k/a_\infty^2 = 9 \times 10^{-9}$ yields (for example) Tu = 0.0387% for $M = 0.2$, 0.0039% for $M = 2.0$, 0.0016% for $M = 5.0$, and 0.0008% for $M = 10.0$. Thus, it perhaps makes better sense when solving over a broad range of Mach numbers to use a fixed Tu (i.e., fixed k/U_∞^2) in the freestream instead of fixed k/a_∞^2); otherwise, higher-Mach-number cases will have an even greater tendency to become laminar.

III. Compressibility Corrections

Wilcox [1] describes many of the compressible-flow closure approximations. A few of them are already employed in most compressible-flow CFD codes. For example, the Reynolds stress tensor of Eq. (4) is already written appropriately for compressible flows. The most commonly used turbulent heat-flux vector closure in the energy equation $q_T = -(\mu_t/Pr_t)\partial h/\partial x_j$ (where h is enthalpy and Pr_t is typically around 0.9 for boundary layers) has been in common use in compressible-flow CFD codes for many years. However, with the models for pressure–diffusion, pressure–dilatation, and pressure–work, they are either under development, very little is known, or proposed models are too complex or have not gained wide acceptance (see, for example, Zeman [14], Grasso and Falconi [15], and Yoshizawa et al. [16]). Many of these compressibility effects are presumed to be small in boundary layers [1]. As a result, most widely used models do not include them. For example, Sarkar's model for the pressure–dilatation correction in compressible flows [17] is rarely employed for boundary-layer computations (see also Wilcox [1] and Grasso and Falconi [15]). In the Sarkar model, the pressure–dilatation adds the following term to the k equation (in the k-ε model):

$$(-\alpha_2\mathcal{P} + \alpha_3\rho\varepsilon)M_T^2 \tag{10}$$

where $\alpha_2 = 0.15$ (0.4 in [15]) and $\alpha_3 = 0.2$.

On the other hand, the Sarkar–Zeman compressibility corrections for dilatation–dissipation are often employed for jets and free-shear mixing layers, in spite of the fact that the reasoning behind them is fundamentally flawed [1] (see also Sarkar [18]). It turns out that dilatation–dissipation is small or negligible, and mixing-layer compressibility effects likely manifest themselves in the pressure–strain redistribution term. Properly formulated corrections are still being explored. In the meantime, the existing dilatation–dissipation corrections provide the desired trends for mixing layers, albeit for the wrong reasons, and so are still considered useful for those cases. It should also be noted that dilatation–dissipation models typically account for the pressure–dilatation correction [19], so when employing both corrections, the coefficient in the dilatation–dissipation model must be reduced by about a factor of 2 from its standard value [15].

Unfortunately, the Sarkar–Zeman compressibility corrections can have a detrimental effect on many boundary-layer predictions (they tend to produce wall skin frictions that are too low and can also negatively impact the size of the predicted separation region [20]). Wilcox [1,21] developed a modification that significantly decreases this detrimental effect, and Brown [22] further attempted to eliminate its potential impact in very-high-Mach-number boundary layers by combining it with the F_1 function of Menter. In the Wilcox correction, the coefficients of the k-ω destruction terms are modified as follows:

$$\beta_c^* = \beta^*[1 + \xi^* F(M_T)] \tag{11}$$

$$\beta_c = \beta - \beta^*\xi^* F(M_T) \tag{12}$$

where

$$F(M_T) = (M_T^2 - M_{T_0}^2)\mathcal{H}(M_T - M_{T_0}) \tag{13}$$

with $\xi^* = 2$, $M_{T_0} = 0.25$, and $\mathcal{H}(\cdot)$ is the Heaviside function.

However, it has been observed[†] that for cold-wall cases, the skin friction is typically overpredicted to such an extent that including a dilatation–dissipation correction can yield improved results, although possibly for the wrong reasons. Zeman [14] noted that the apparent unimportance of the pressure–dilatation and dilatation–dissipation in boundary layers is "only a question of degree." He found that as freestream Mach number increases and wall cooling increases, compressibility effects become increasingly important. In the Zeman dilatation–dissipation correction for boundary layers, the coefficients of the k-ω destruction terms are modified as in Eqs. (11) and (12), only now $F(M_T)$ is given by

$$F(M_T) = \left[1 - \exp\left(-\left(\frac{M_T - M_{T_0}}{\Lambda}\right)^2\right)\right]\mathcal{H}(M_T - M_{T_0}) \tag{14}$$

with $\xi^* = 0.75$, $M_{T_0} = 0.2$, and $\Lambda = 0.66$.

In addition to a pressure–dilatation correction and a dilatation–dissipation correction, Grasso and Falconi [15] also included a correction to the k equation in their k-ε model, due to the scalar product of the Favre velocity and the mean pressure gradient. They believed that this term may be influential in regions of large pressure and density gradients.

Both Wilcox [1] and Huang et al. [23] mentioned that the k-ε form of the two-equation model exhibits more deviation from the compressible law-of-the-wall than k-ω at high Mach numbers. Wilcox [1] also pointed out that the k-ε form is more problematic for adverse pressure-gradient wall-bounded flows. Huang et al. [23] proposed a possible iterative procedure to reproduce the expected profile and also mentioned that alternative forms such as k-$(\varepsilon^{5/6}/k)$ may reduce the sensitivity, but neither of these proposals was widely used.

Catris and Aupoix [24] extended the analysis of Huang et al. [23] and showed that specific corrections to the diffusion terms are necessary to make the models consistent with the logarithmic law for compressible boundary layers. The corrections were derived for a variety of models. Here, we are only concerned with the k-ω form. For example, the diffusion terms of Eqs. (1) and (2) get altered as follows:

$$\frac{\partial}{\partial x_j}\left[\frac{1}{\rho}(\mu + \sigma_k\mu_t)\frac{\partial(\rho k)}{\partial x_j}\right] \tag{15}$$

[†]Private communication with J. A. White, 2008.

$$\frac{\partial}{\partial x_j}\left[\frac{1}{\sqrt{\rho}}(\mu+\sigma_\omega\mu_t)\frac{\partial(\sqrt{\rho}\omega)}{\partial x_j}\right] \tag{16}$$

However, Catris and Aupoix [24] pointed out that for k-ω, the difference in results due to modifying the diffusion terms is only very slight. This further confirms the low sensitivity of k-ω to compressibility effects in boundary-layer flow, as described in [1,23].

A length-scale modification was proposed by Vuong and Coakley [25] and Huang and Coakley [26] to reduce the magnitude of heat transfer for high-speed separated boundary layers near reattachment (see also Brown [22] and Coratekin et al. [27]). In this correction, the length scale going into the eddy viscosity is limited based on Bradshaw's relation $\tau_{ij}/\rho \propto a_1 k$ and the mixing-length relation $\ell = \kappa d$. The turbulent length scale is limited by

$$\ell = \min\left(\kappa d\sqrt{a_1}; \frac{\sqrt{k}}{\omega}\right) \tag{17}$$

(Note that in Vuong and Coakley [25] and Huang and Coakley [26], there is an additional factor of $C_\mu = 0.09$ present, due to the different way that ω is defined.) Because $\omega = \sqrt{k}/\ell$, the end result is that the eddy viscosity is limited according to

$$\mu_t = \min(\mu_{t,\text{std}}; \rho\kappa d\sqrt{a_1 k}) \tag{18}$$

where $\mu_{t,\text{std}}$ is the eddy viscosity computed the usual way. It should be noted here that the assumption of constant turbulent Prandtl number has been recently questioned, relative to its effect on heat flux for shock/boundary-layer cases [28]. A variable turbulent Prandtl number model was shown to improve heat flux near reattachment.

A rapid compression fix was implemented by Coakley and Huang [29] (see also Vuong and Coakley [25], Coratekin et al. [27], and Forsythe et al. [30]). In this fix, the production term in the ω equation,

$$\frac{\alpha\rho}{\mu_t}\mathcal{P} = -\frac{\alpha\rho}{\mu_t}\tau_{ij}\frac{\partial u_i}{\partial x_j} = \alpha\rho\bar{S}^2 - \frac{2}{3}\alpha\rho\omega\frac{\partial u_k}{\partial x_k} \tag{19}$$

is altered to read

$$\frac{\alpha\rho}{\mu_t}\mathcal{P} = \alpha\rho\bar{S}^2 - \frac{4}{3}\rho\omega\frac{\partial u_k}{\partial x_k} \tag{20}$$

where

$$\bar{S}^2 \equiv \left(\frac{\partial u_i}{\partial x_j}+\frac{\partial u_j}{\partial x_i}-\frac{2}{3}\frac{\partial u_k}{\partial x_k}\delta_{ij}\right)\frac{\partial u_i}{\partial x_j} = \left(\frac{\partial u_i}{\partial x_j}+\frac{\partial u_j}{\partial x_i}\right)\frac{\partial u_i}{\partial x_j} - \frac{2}{3}\left(\frac{\partial u_k}{\partial x_k}\right)^2 = S^2 - \frac{2}{3}\left(\frac{\partial u_k}{\partial x_k}\right)^2 \tag{21}$$

or, equivalently,

$$\bar{S}^2 = 2\bar{S}_{ij}\bar{S}_{ij} \tag{22}$$

where

$$\bar{S}_{ij} = S_{ij} - \frac{1}{3}\frac{\partial u_k}{\partial x_k}\delta_{ij} \tag{23}$$

Thus, in this rapid compression fix, the original $(2/3)\alpha$ (which is close to $1/3$) gets increased to a fixed value of $4/3$ for linear deformations.

This modification was made in order to increase the size of computed separation-bubble regions, by ensuring that the turbulent length scale does not change too quickly when undergoing rapid compression. However, as discussed in Forsythe et al. [30], the shear-stress transport part of the Menter SST model already improves correlations with experimental bubble size, so the ad hoc rapid compression fix was not used for that model. The Wilcox06 model is designed with a similar stress limiter modification, so this model, too, probably would not benefit from the rapid compression fix.

In summary, when considering high-Mach-number compressible boundary-layer flows using k-ω models, the conservation of total energy should be configured to include the contribution of the turbulent kinetic energy k, and the mean flow energy equation should include the molecular and turbulent diffusion of k. It is sometimes common practice to ignore these effects, which is certainly justified when k is significantly smaller than the square of the mean velocity. Furthermore, turbulent production should officially include the $(2/3)\rho k$ term, which multiplies $\partial u_k/\partial x_k$ and hence is identically zero for incompressible flows. Because this term typically has little effect over a broad range of conditions, it is sometimes ignored, particularly when other approximations, limiting, etc., are employed for turbulence production. Other than these considerations (which may or may not be important, depending on the case), little extra appears to be called for (based on the currently available literature) in terms of specific corrections for compressible Navier–Stokes codes applied to boundary-layer flows. Adopting the modified diffusion-term form of Catris and Aupoix [24] has been shown to make very little difference for k-ω models. The length-scale modification of Vuong and Coakley [25] appears to only be important for the specific circumstance of predicting heat transfer near reattachment after separation, but this flow feature may also be improved by adopting models with variable turbulent Prandtl number. The rapid compression fix of Coakley and Huang [29] has been negated by the more accepted stress limiters that appear in SST and Wilcox06.

However, Zeman [14] and practical experience indicate that the need for corrections in hypersonic boundary layers becomes increasingly evident as Mach number increases, particularly for cold walls. But the traditional Sarkar–Zeman–Wilcox fixes for free-shear flows tend to overcorrect in many cases when applied to boundary-layer flows. In the Results section, the influence of the less widely used Zeman correction (formulated for boundary-layer flows) is explored.

IV. Results

In order to test the ability of k-ω turbulence models to predict compressible boundary-layer flow, computations were performed for flow over a flat plate in zero pressure gradient for a variety of flow conditions. Most of the computations were performed using the CFL3D code [13]. Note that in CFL3D, the turbulence models are decoupled from the mean flow equations, k is *not* included in the definition of total energy, and diffusion of k does not appear in the mean flow energy equation for its models tested here. Furthermore, for the current applications, Eq. (7) is used for production, with the $(2/3)\rho k$ term ignored. (Some computations were tried with this term included, and it was found to make little difference even for $M = 10$ cases.) The $(2/3)\rho k$ term was also neglected in τ_{ij} [Eq. (4)]. For comparison, several results were also obtained using the VULCAN code [31], in which the turbulence models are fully coupled to the mean flow equations and no approximations are made for τ_{ij} or the turbulence production terms.

The majority of runs were performed using the Menter SST model. Full Navier–Stokes equations (as opposed to thin-layer) were employed. For subsonic Mach numbers, the inflow boundary condition set total pressure and total temperature conditions (according to the particular Mach number). The pressure was extrapolated from the interior of the domain, and the remaining variables were determined from the extrapolated pressure and the input data using isentropic relations. The outflow boundary condition set $p/p_\infty = 1$ and extrapolated all other quantities from the interior of the domain. For supersonic Mach numbers, the inflow boundary condition set all primitive variables, and the outflow boundary condition extrapolated all variables from the interior of the domain. In all cases, the top boundary, located a nondimensional distance $y = 1$ from the wall, used a far-field Riemann invariant boundary condition. The wall boundary condition enforced no slip and set temperature either 1) according to a desired T_w/T_∞ or 2) according to $T_w = T_{\text{aw,ideal}}$, where $T_{\text{aw,ideal}}$ is the ideal adiabatic-wall temperature computed from $T_{\text{aw,ideal}} = T_\infty(1 + \frac{1}{2}(\gamma-1)M^2)$. The latter method yielded almost the same results as enforcing zero wall-temperature gradient, which

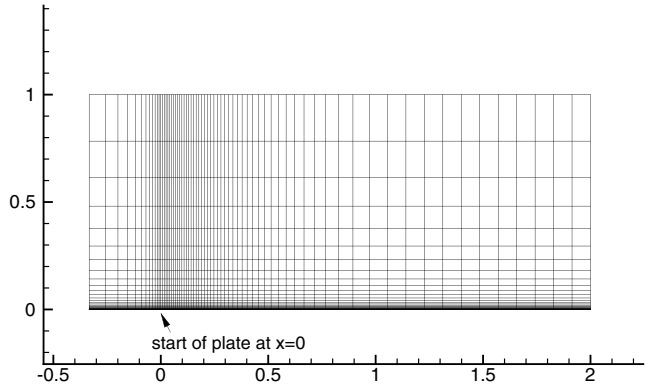

Fig. 1 Flat-plate grid with every fourth grid point removed in each coordinate direction for clarity.

ensured no heat flux at the wall. The freestream T_∞ was taken to be 540 R.

As mentioned earlier, the wall boundary conditions for turbulent quantities were those recommended by Menter [8]. Although not shown, the boundary condition on ω_w was varied by a factor of 10 in both directions, but this change did not have an appreciable influence on the results. The far-field boundary conditions for turbulent quantities were determined from Tu $= 0.08165\%$ and $\mu_{t,\infty}/\mu_\infty = (2 \times 10^{-7})Re$. For the results to be shown, $Re = 10^7$ over the length of a plate two nondimensional units long. Thus, Re per unit length was 5×10^6 and $\mu_{t,\infty}/\mu_\infty = 1.0$.

The finest grid employed was 273×193, with 225 points on the plate and 49 points leading up to the plate (where symmetry was imposed). Nondimensional minimum normal spacing at the wall was approximately $\Delta y = 1 \times 10^{-6}$, yielding average $y^+ = 0.2$ (or less for higher Mach numbers). There was streamwise clustering near the plate leading edge, as shown in Fig. 1, for which only every fourth grid point is shown for clarity. For supersonic Mach number cases, it was necessary to employ a flux limiter in the computations.

Table 1 summarizes the cases computed. For the purposes of this study, the wall temperature is defined as hot or cold, depending on whether it is above or below the ideal adiabatic-wall temperature. Note that the $M = 2$ and $T_w/T_\infty = 2$ case is only slightly hot, with wall temperature only slightly above adiabatic.

A grid study for the $M = 5$ adiabatic-wall case was conducted using the SST model on the 273×193 (fine grid), along with two successively coarser grids for which every other grid point was removed in each coordinate direction (medium is 137×97 and coarse is 69×49). Results are shown in Fig. 2. The biggest differences were near the plate leading edge, where the predicted transition locations differ, particularly for the coarse level. But over most of the plate, the medium and fine grids yielded very close results. The coarse grid was not in the asymptotic range, but assuming second-order convergence on the medium and fine grids, Richardson extrapolation can be used to find the error. For example, at $Re_x = 5.275 \times 10^6$, the fine-grid error was less than one-tenth of 1%, and the grid convergence index [32] was GCI $= 0.18\%$ (using a factor of safety of 3).

Table 1 Flat-plate cases computed

Mach	T_w/T_∞	$T_w/T_{\text{aw,ideal}}$	Wall type
0.2	1.008	1.0	Adiabatic
5.0	6.0	1.0	Adiabatic
10.0	21.0	1.0	Adiabatic
0.2	5.0	4.96	Hot
2.0	1.0	0.556	Cold
2.0	2.0	1.11	Hot
5.0	1.0	0.167	Cold
5.0	3.0	0.5	Cold
5.0	20.0	3.33	Hot
10.0	1.0	0.0476	Cold
10.0	10.0	0.476	Cold
10.0	40.0	1.905	Hot

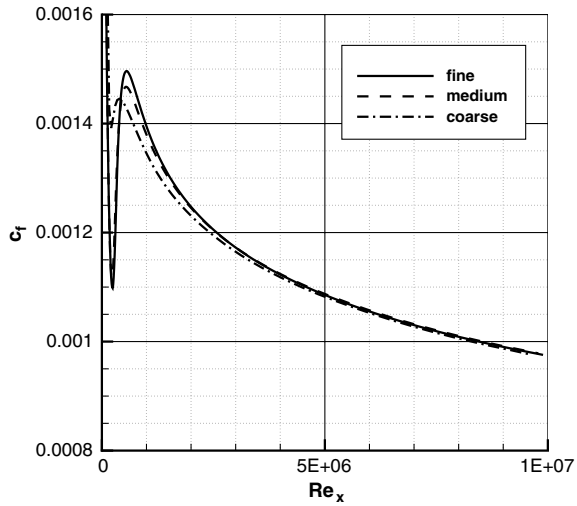

Fig. 2 Wall skin-friction coefficient grid study for $M = 5$, adiabatic wall, using SST on three successive grid sizes.

In order to get an idea about the magnitude of the computed turbulent kinetic energy relative to the square of the velocity, profiles of local k/U_∞^2 are shown as a function of y in the boundary layer at the x location where $Re_x = 5 \times 10^6$ for several different cases in Fig. 3a. The maximum level was only about 3%. Figure 3b shows the value of another quantity sometimes used to ascertain the compressibility effects of turbulence (albeit most commonly for free-shear-layer applications) [19], the turbulence Mach number M_T. The highest levels in the boundary layer at a given freestream Mach number occur for the cold-wall cases. For example, for $M = 10$ and $T_w/T_\infty = 1$, the peak M_T reaches approximately 0.5.

The Appendix reviews several correlations for compressible skin friction and heat transfer on a flat plate. Although there have been many developed, the current paper primarily focuses on two (the van Driest and Spalding–Chi correlations) to give an indication of the uncertainty inherent at some conditions. Most results to follow focus on wall skin friction. As discussed in the Appendix, the wall heat flux for nonadiabatic walls is proportional to the skin friction through the so-called Reynolds analogy. In other words, if the wall skin friction is predicted too high, then the Stanton number will typically also be proportionally too high.

Results for the adiabatic-wall cases using the finest grid are shown in comparison with van Driest and Spalding–Chi correlations in Fig. 4. For these cases, the two theories agree well with each other. The CFD results captured the correct trends compared to theory, although the tendency of numerically induced transition in the CFD to occur further aft with increasing Mach number should be noted [33]. Compared to the correlations, the SST model slightly underpredicted turbulent skin friction for the subsonic Mach number case and overpredicted the correlations for the hypersonic Mach numbers. The Wilcox06 model produced similar C_f as SST for all three cases, although it had a greater tendency to remain laminar than SST as the Mach number increased. (Although not shown, increasing freestream Tu could shift the transition location for Wilcox06 forward.) The Wilcox06 model is also known to suffer from some dependence on the freestream value of the ω boundary condition, whereas SST does not [34].

Effects of a different code (VULCAN with SST model), as well as effects of including two different compressibility corrections, are shown in Fig. 5. The VULCAN results are seen to be relatively close to the CFL3D results on the same grid, yielding slightly lower C_f levels. Regarding the compressibility corrections, generally speaking, for adiabatic wall with freestream $M \leq 10$ there is only a fairly small influence on the results. Both the Wilcox and the Zeman corrections reduce the skin friction, with the Wilcox correction having the larger effect. Note that Wilcox [1] reported a larger decrease in C_f with the Zeman correction, because he used different coefficients (his version of the Zeman model was designed for free-shear flows).

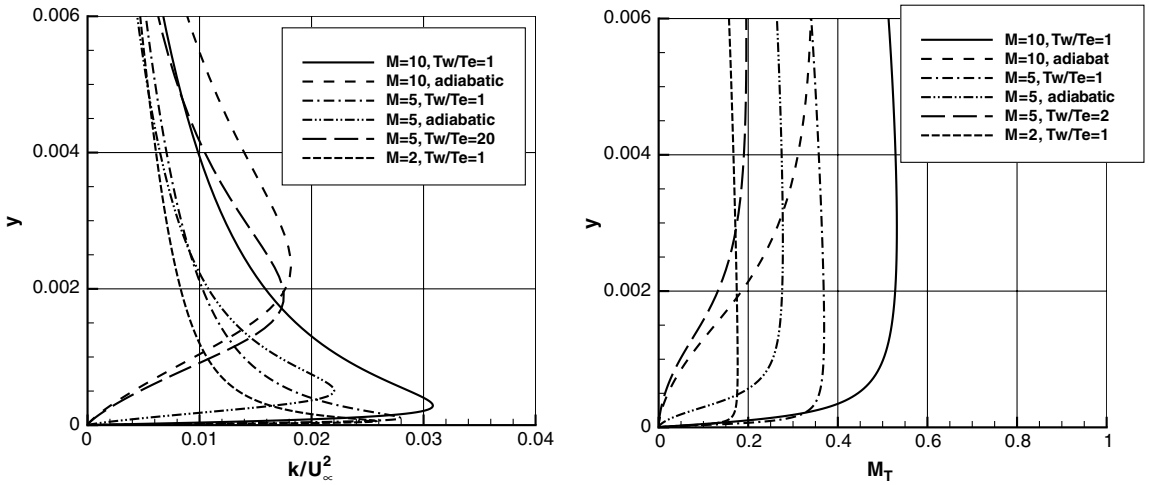

Fig. 3 Profiles of local turbulent quantities in the boundary layer at $Re_x = 5 \times 10^6$, SST model: a) k/U_∞^2 and b) $M_T = (\sqrt{2k})/a$.

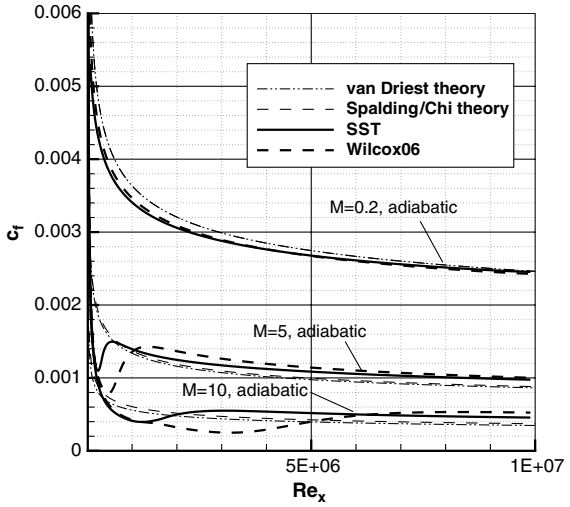

Fig. 4 Wall skin-friction coefficients for adiabatic-wall cases.

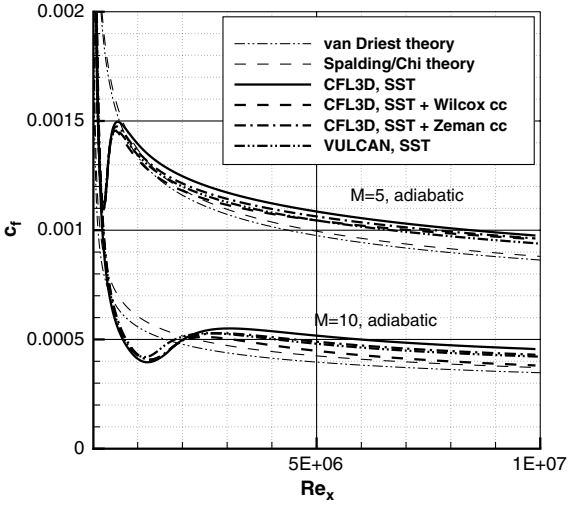

Fig. 5 Effect of code and Wilcox–Zeman compressibility corrections on wall skin-friction coefficients for adiabatic-wall cases.

Results for two cold-wall cases are shown in Fig. 6 (heat transfer coefficients are shown here in addition to skin-friction coefficients for CFL3D in order to demonstrate that the two quantities are roughly proportional). For these cases, the van Driest and Spalding–Chi correlations differ significantly, as indicated by the shaded bands. According to Hopkins and Inouye [35], given limited directly measured experimental data, the van Driest correlation is believed to be better than Spalding–Chi for $T_w/T_{\text{aw}} > 0.3$, but neither theory predicts C_f reliably at lower wall temperatures. In Fig. 6, T_w/T_{aw} is smaller than 0.3, so the shaded bands here represent some measure of uncertainty at these conditions. Again, both CFL3D and VULCAN (using SST) yield skin-friction levels that are very close. These SST results are significantly high in comparison with the correlations.

It is generally well known that simple algebraic turbulence models such as Baldwin–Lomax [36] can perform reasonably well for attached hypersonic boundary-layer flows, provided that the definition of y^+ in the van Driest damping function uses local values for ρ and μ (rather than wall values) [37], as follows: $y^+ = \sqrt{(\rho\tau_w)}y/\mu$. This local definition is particularly important for cold-wall cases because of large temperature gradients near the wall. At a given distance from the wall, the local formulation decreases the van Driest damping function and hence decreases the eddy viscosity. From the discussion in Dilley [37], it is not clear whether the good agreement is a result of sound physics or luck, although it is noted that the local formulation is included in the algebraic model of Cebeci and Smith [38]. As shown here, using this version of Baldwin–Lomax for the two cold-wall cases yields better predictions than SST, in reasonably good agreement with the van Driest correlation. Employing SST with the Wilcox compressibility correction (SST+ Wilcox cc) lowers skin friction significantly. Both CFL3D and VULCAN produce nearly identical results. Although results still lie within the band defined by the two correlations, the SST + Wilcox cc results are quite a bit lower than those of Baldwin–Lomax. Results with the Zeman correction agree better with Baldwin–Lomax results and the van Driest correlation. As shown in Fig. 7, the Baldwin–Lomax model and SST + Zeman cc produce lower eddy viscosity values than uncorrected SST very near the wall (corresponding to $y^+ < O(100)$). The lower levels produce a less turbulent profile and, consequently, lower wall skin friction.

Results for two hot-wall cases are shown in Fig. 8. As for the cold-wall cases, the two correlations differ significantly. However, as mentioned in Spalding and Chi [39], high-Mach-number experiments with $T_w/T_{\text{aw}} > 1$ are far rarer than cooled walls. Therefore, it is difficult to know with certainty which correlation is better. In these cases, the results using SST generally fell within the shaded band defined by the two correlations; for $M = 0.2$ and $T_w/T_\infty = 5$, results were closer to the van Driest correlation, and for $M = 5$ and $T_w/T_\infty = 20$, results were closer to the Spalding–Chi correlation. As expected for these cases, the compressibility corrections made almost no difference in the results, because the M_T is relatively low, as shown in Fig. 3b.

CFD results using the SST model (without and with the Zeman compressibility correction) for various cases in terms of the ratio $C_f/C_{f,\text{incomp}}$ are overplotted alongside the van Driest and Spalding–

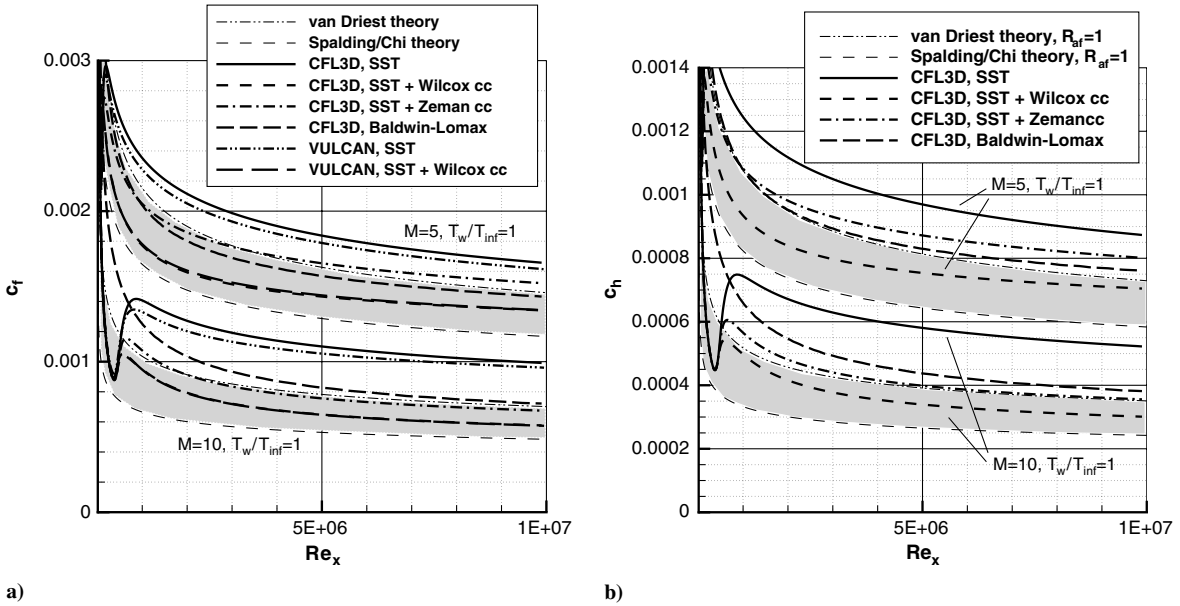

a) b)

Fig. 6 Two cold-wall cases; a) wall skin-friction coefficient and b) wall heat transfer coefficient.

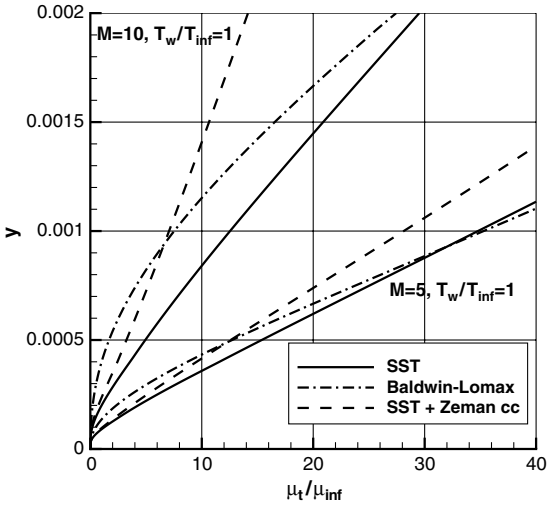

Fig. 7 Profiles of nondimensional μ_t for $M = 5$ and $M = 10$ cases, $T_w/T_\infty = 1$, at $Re_x = 5 \times 10^6$.

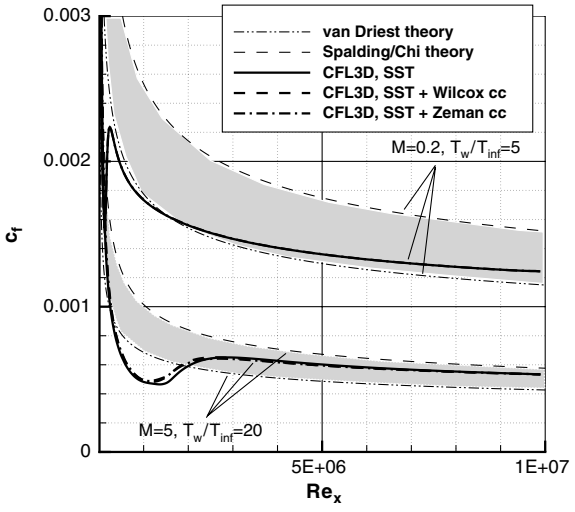

Fig. 8 Wall skin-friction coefficients for two hot-wall cases.

Chi correlations for $Re_x = 5 \times 10^6$ in Figs. 9a and 9b. In all cases, the $C_{f,\text{incomp}}$ used was the CFD result for $M = 0.2$ with adiabatic-wall temperature. The trends discussed above can be clearly discerned in this plot. Although, overall, the general effects of Mach number and wall temperature on skin friction can be *qualitatively* predicted by SST with no explicit compressibility correction, adiabatic- and cold-wall cases are consistently overpredicted *quantitatively* as Mach number is increased (up to about 30% at $M = 10$ for adiabatic walls and up to as much as 40–100% at $M = 10$ for cold walls). SST results using the Zeman compressibility correction are significantly closer to the correlations. On the other hand, hot-wall cases yielded results that lay in or near the band defined by the two correlations, and the compressibility correction made little difference.

Results can also be plotted as a function of $T_w/T_{\text{aw,ideal}}$. Figure 10 shows van Driest and Spalding–Chi correlations for both $M = 5$ and 10, along with current SST results. The SST results with no compressibility correction mostly lie above the shaded regions defined by the two correlations, except for the hot-wall cases, in which results start to fall below the Spalding–Chi correlation. When the Zeman compressibility correction is employed, cold-wall results are improved relative to the correlations, whereas hot-wall results are essentially not changed at all.

V. Conclusions

The most widely used compressibility corrections for k-ω models for high-Mach-number boundary-layer flows are based on improvements intended for free-shear applications. As such, these corrections are often unacceptable for boundary-layer flows, and many researchers prefer to employ no corrections at all. Although it should be borne in mind that there is some uncertainty in the theoretical correlations (especially at Mach numbers well above 5), it appears that the uncorrected k-ω models perform progressively worse (particularly for cold walls) as the Mach number is increased in the hypersonic regime. As is well known, simple algebraic models such as Baldwin–Lomax perform better compared to experiment and correlations in these circumstances.

There is still no clarity about whether dilatation–dissipation and pressure–dilatation effects are important in boundary layers or not, particularly at the higher Mach numbers and for cold-wall hypersonic cases. Anything that reduces near-wall eddy viscosity in these situations can help obtain better agreement with correlations, but there is currently no strong physical argument for choosing one fix over another. Corrections designed for improving free-shear flows tend to overcorrect in the boundary layer and yield wall skin friction (and heat transfer) values that are too low. In this paper, it was

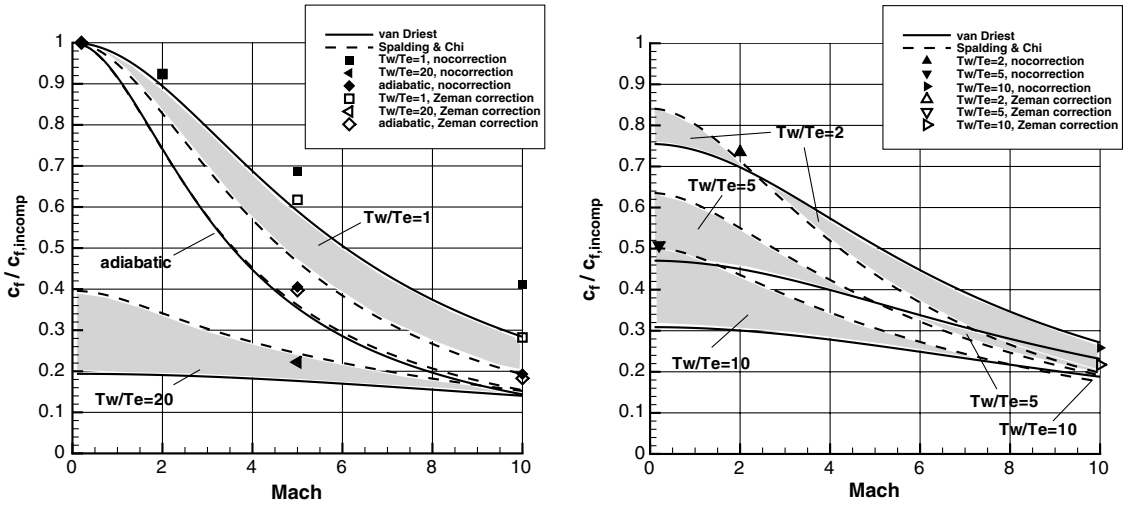

Fig. 9 Theoretical compressible wall skin friction compared to incompressible level as a function of Mach number for $Re_x = 5 \times 10^6$, $T_e = 540$ R, including SST (no compressibility correction), and SST (Zeman compressibility correction): a) $T_w/T_e = 1, 20$, and adiabatic and b) $T_w/T_e = 2, 5$, and 10.

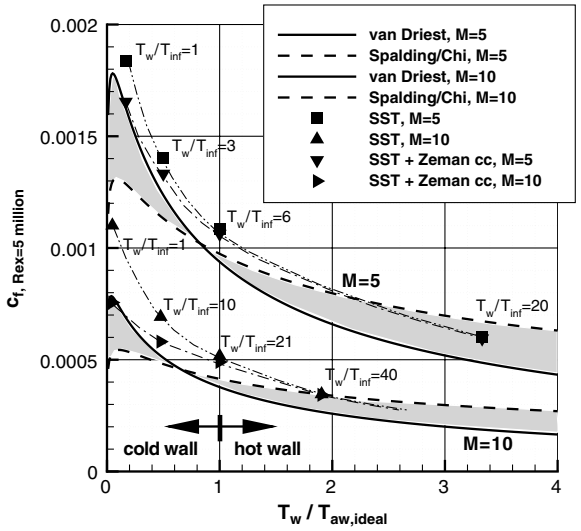

Fig. 10 Compressible wall skin friction as a function of $T_w/T_{\mathrm{aw,ideal}}$ for $Re_x = 5 \times 10^6$ and $T_e = 540$ R, with SST results included.

shown that a dilatation–dissipation correction designed by Zeman specifically for use in boundary-layer flows works reasonably well for cold-wall cases. Its influence in the boundary layer is smaller than that of the popular Wilcox correction.

The physical modeling needed to improve wall skin-friction predictions in highly compressible boundary-layer flows has yet to be formulated and accepted for k-ω turbulence models. Currently, omitting explicit compressibility corrections works reasonably well only for lower Mach numbers (e.g., $M < 5$) or for hot-wall cases. Using the Zeman compressibility correction (formulated for boundary layers) improves high-Mach-number cold-wall results, but it would be an insufficient correction for free-shear flows. In other words, a recommendation cannot be made for a single form of compressibility correction that works well for both cold-wall boundary layers and free-shear flows. Better overall physics-based compressible turbulence modeling is clearly needed.

Appendix: Experimental Correlations for Skin Friction and Heat Transfer on a Flat Plate

Wall skin friction is given by the formula

$$C_f = \frac{\tau_w}{2\rho_e U_e^2} \tag{A1}$$

where τ_w is the wall shear stress $\mu_w \partial u/\partial y|_w$ and the subscript e represents edge or freestream values. There have been a plethora of correlations for wall skin friction (and heat transfer) for the flat plate over the years (see, for example, White [40], Peterson [41], and Hopkins and Inouye [35]). One of the reasons for the large number is the fact that there is a significant amount of scatter in the available experimental data, especially those with heat transfer, making certainty difficult. Many of the skin-friction correlations use a compressibility transformation idea:

$$C_f = \frac{1}{F_c} C_{f,\mathrm{incomp}}(Re_\theta F_{Re_\theta}) \tag{A2}$$

In other words, the formula for incompressible $C_{f,\mathrm{incomp}}$, which is often expressed as a function of Re_θ, is instead computed using the altered variable $Re_\theta F_{Re_\theta}$ and then divided by the function F_c. A widely used correlation for $C_{f,\mathrm{incomp}}$ is the Karman–Schoenherr relation (see Roy and Blottner [42]):

$$C_{f,\mathrm{incomp}} = \frac{1}{\log_{10}(2Re_\theta)[17.075\log_{10}(2Re_\theta) + 14.832]} \tag{A3}$$

Here, three correlations for C_f are described: van Driest [43] (often referred to as van Driest II), Spalding and Chi [39], and White and Christoph [44]. For each of these, the F_c is defined the same way:

$$F_c = \frac{T_{\mathrm{aw}}/T_e - 1}{(\sin^{-1}A + \sin^{-1}B)^2} \tag{A4}$$

where T_e represents the edge or freestream temperature, and

$$T_{\mathrm{aw}} = T_e\left(1 + r\frac{\gamma - 1}{2}M^2\right) \tag{A5}$$

The recovery factor r is taken to be 0.9. This empirical factor is often introduced because, in practice, energy recovery is not perfect. The numerator of Eq. (A4) is thus simply $\frac{1}{2}r(\gamma - 1)M^2$. The A and B are given by

$$A = \frac{2a^2 - b}{(b^2 + 4a^2)^{1/2}} \tag{A6}$$

$$B = \frac{b}{(b^2 + 4a^2)^{1/2}} \tag{A7}$$

where

$$a = \left(r \frac{\gamma - 1}{2} M^2 \frac{T_e}{T_w} \right)^{1/2} \tag{A8}$$

$$b = \frac{T_{\text{aw}}}{T_w} - 1 = \frac{T_e}{T_w} \left(1 + r \frac{\gamma - 1}{2} M^2 \right) - 1 \tag{A9}$$

The three correlations differ in their definitions of F_{Re_θ}.
van Driest:

$$F_{Re_\theta} = \frac{\mu_e}{\mu_w} \tag{A10}$$

Spalding and Chi:

$$F_{Re_\theta} = \left(\frac{T_w}{T_e} \right)^{-0.702} \left(\frac{T_{\text{aw}}}{T_w} \right)^{0.772} \tag{A11}$$

White and Christoph:

$$F_{Re_\theta} = \sqrt{F_c} \left(\frac{\mu_e}{\mu_w} \right) \left(\frac{T_e}{T_w} \right)^{1/2} \tag{A12}$$

(Note the typographical error in White [40] in Table 7-3, where the term Q is inverted.) Both van Driest and White–Christoph correlations are functions of μ_e/μ_w. This quantity can be obtained via Sutherland's law (see White [40]):

$$\mu = \mu_0 \left(\frac{T}{T_0} \right)^{3/2} \frac{T_0 + S'}{T + S'} \tag{A13}$$

where for air $\mu_0 = 0.1716$ mP, $T_0 = 491.6$ R, and $S' = 199$ R. Thus,

$$\frac{\mu_e}{\mu_w} = \left(\frac{T_w}{T_e} \right)^{-3/2} \frac{(T_w/T_e) + (S'/T_e)}{1 + (S'/T_e)} \tag{A14}$$

Therefore, when Sutherland's law is used, both of these correlations are functions not only of the ratio T_w/T_e, but also of the freestream temperature T_e itself. For all of the work herein, T_e is chosen to be 540 R.

Using Eq. (A3) for the $C_{f,\text{incomp}}$ value, results for the compressible C_f can be computed for each of the correlations. For the adiabatic-wall case (for which the most experimental data exist), all correlations give nearly the same result. For fixed wall-temperature ratios, it turns out that results using van Driest and White–Christoph are very similar, but results using Spalding–Chi can differ significantly. Spalding and Chi [45] claim a smaller root mean square error compared to van Driest [43] using a variety of experiments, but recall that relatively few experiments exist for walls with heat transfer. The main point here is that there is some uncertainty regarding C_f for walls with heat transfer, so it is more difficult to validate (or invalidate) turbulence models for these cases with confidence. In the literature, most people tend to compare with the van Driest correlation, but others have since developed correlations that may work better in specific cases. For example, Huang et al. [46] developed a method for which skin friction for strongly cooled walls falls below van Driest, in better agreement with data.

The wall heat flux is often expressed [40] in terms of the Stanton number:

$$St = C_h = \frac{q_w}{\rho_e U_e c_p (T_w - T_e)} \tag{A15}$$

where the heat flow at the wall $q_w = -k(\partial T/\partial y)|_w$. For nonadiabatic walls, the so-called Reynolds analogy is usually used to relate the local wall heat flux in terms of skin friction:

$$St \approx \tfrac{1}{2} C_f R_{\text{af}} \tag{A16}$$

where R_{af} is the Reynolds analogy factor. This factor generally lies in the range $0.9 < R_{\text{af}} < 1.3$ and is believed to be close to unity for hypersonic flows [42] and for very cold walls [20]. Thus, St is directly proportional to C_f, at approximately one-half of its numerical value.

References

[1] Wilcox, D. W., *Turbulence Modeling For CFD*, 3rd ed., DCW Industries, La Canada, CA, 2006.

[2] Morkovin, M., "Effects of Compressibility on Turbulent Flows," *Mecanique de la Turbulence*, edited by A. Favre, Gordon and Breach, New York, 1962, pp. 367–380.

[3] So, R. M. C., Gatski, T. B., and Sommer, T. P., "Morkovin Hypothesis and the Modeling of Wall-Bounded Compressible Turbulent Flows," *AIAA Journal*, Vol. 36, No. 9, 1998, pp. 1583–1592. doi:10.2514/2.584

[4] Sarkar, S., Erlebacher, G., Hussaini, M. Y., and Kreiss, H. O., "The Analysis and Modeling of Dilatational Terms in Compressible Turbulence," NASA CR-181959, 1989.

[5] Aupoix, B., "Modelling of Compressibility Effects in Mixing Layers," *Journal of Turbulence*, Vol. 5, 2004, Article N7. doi:10.1088/1468-5248/5/1/007

[6] Abdol-Hamid, K. S., Pao, S. P., Massey, S. J., and Elmiligui, A., "Temperature Corrected Turbulence Model for High Temperature Jet Flow," *Journal of Fluids Engineering*, Vol. 126, No. 5, 2004, pp. 844–850. doi:10.1115/1.1792266

[7] Wilcox, D. W., "Formulation of the k-ω Turbulence Model Revisited," *AIAA Journal*, Vol. 46, No. 11, 2008, pp. 2823–2838. doi:10.2514/1.36541

[8] Menter, F. R., "Two-Equation Eddy-Viscosity Turbulence Models for Engineering Applications," *AIAA Journal*, Vol. 32, No. 8, 1994, pp. 1598–1605. doi:10.2514/3.12149

[9] Baurle, R. A., "Modeling of High Speed Reacting Flows: Established Practices and Future Challenges," AIAA Paper 2004-267, Jan. 2004.

[10] Morrison, J. H., "Flux Difference Split Scheme for Turbulent Transport Equations," AIAA Paper 90-5251, Oct. 1990.

[11] Menter, F. R., "Improved Two-Equation k-omega Turbulence Models for Aerodynamic Flows," NASA TM-103975, Oct. 1992.

[12] Spalart, P. R., and Rumsey, C. L., "Effective Inflow Conditions for Turbulence Models in Aerodynamic Calculations," *AIAA Journal*, Vol. 45, No. 10, 2007, pp. 2544–2553. doi:10.2514/1.29373

[13] Krist, S. L., Biedron, R. T., and Rumsey, C. L., "CFL3D User's Manual (Version 5.0)," NASA TM-1998-208444, June 1998.

[14] Zeman, O., "A New Model for Supersonic/Hypersonic Turbulent Boundary Layers," AIAA Paper 93-0897, Jan. 1993.

[15] Grasso, F., and Falconi, D., "High-Speed Turbulence Modeling of Shock-Wave/Boundary-Layer Interaction," *AIAA Journal*, Vol. 31, No. 7, 1993, pp. 1199–1206. doi:10.2514/3.49062

[16] Yoshizawa, A., Liou, W. W., Yokoi, N., and Shih, T.-H., "Modeling of Compressible Effects on the Reynolds Stress Using a Markovianized Two-Scale Method," *Physics of Fluids*, Vol. 9, No. 10, 1997, pp. 3024–3036. doi:10.1063/1.869412

[17] Sarkar, S., "The Pressure-Dilatation Correlation in Compressible Flows," *Physics of Fluids A*, Vol. 4, No. 12, 1992, pp. 2674–2682. doi:10.1063/1.858454

[18] Sarkar, S., "The Stabilizing Effect of Compressibility in Turbulent Shear Flow," *Journal of Fluid Mechanics*, Vol. 282, 1995, pp. 163–186. doi:10.1017/S0022112095000085

[19] Chassaing, P., Antonia, R. A., Anselmet, F., Joly, L., and Sarkar, S., *Variable Density Fluid Turbulence*, Kluwer Academic, Dordrecht, The Netherlands, 2002.

[20] MacLean, M., Wadhams, T., Holden, M., and Johnson, H., "A Computational Analysis of Ground Test Studies of the HIFiRE-1 Transition Experiment," AIAA Paper 2008-0641, Jan. 2008.

[21] Wilcox, D. C., "Progress in Hypersonic Turbulence Modeling," AIAA Paper 91-1785, June 1991.

[22] Brown, J., "Turbulence Model Validation for Hypersonic Flows," AIAA Paper 2002-3308, June 2002.

[23] Huang, P. G., Bradshaw, P., and Coakley, T. J., "Turbulence Models for Compressible Boundary Layers," *AIAA Journal*, Vol. 32, No. 4, 1994, pp. 735–740. doi:10.2514/3.12046

[24] Catris, S., and Aupoix, B., "Density Corrections for Turbulence Models," *Aerospace Science and Technology*, Vol. 4, 2000,

pp. 1–11.
doi:10.1016/S1270-9638(00)00112-7
[25] Vuong, S. T., and Coakley, T. J., "Modeling of Turbulence for Hypersonic Flows with and Without Separation," AIAA Paper 87-0286, Jan. 1986.
[26] Huang, P. G., and Coakley, T. J., "Turbulence Modeling for Complex Hypersonic Flows," AIAA Paper 93-0200, Jan. 1993.
[27] Coratekin, T., van Keuk, J., and Ballmann, J., "Performance of Upwind Schemes and Turbulence Models in Hypersonic Flows," *AIAA Journal*, Vol. 42, No. 5, 2004, pp. 945–957.
doi:10.2514/1.9588
[28] Xiao, X., Hassan, H. A., Edwards, J. R., and Gaffney, R. L., Jr., "Role of Turbulent Prandtl Numbers on Heat Flux at Hypersonic Mach Numbers," *AIAA Journal*, Vol. 45, No. 4, 2007, pp. 806–813.
doi:10.2514/1.21447
[29] Coakley, T. J., and Huang, P. G., "Turbulence Modeling for High Speed Flows," AIAA Paper 92-0436, Jan. 1992.
[30] Forsythe, J. R., Hoffmann, K. A., and Damevin, H.-M., "An Assessment of Several Turbulence Models for Supersonic Compression Ramp Flow," AIAA Paper 98-2648, June 1998.
[31] White, J. A., and Morrison, J. H., "Pseudo-Temporal Multi-Grid Relaxation Scheme for Solving the Parabolized Navier–Stokes Equations," AIAA Paper 99-3360, June 1999.
[32] Roache, P. J., *Verification and Validation in Computational Science and Engineering*, Hermosa, Albuquerque, NM, 1998.
[33] Rumsey, C. L., and Spalart, P. R., "Turbulence Model Behavior in Low Reynolds Number Regions of Aerodynamic Flowfields," AIAA Paper 2008-4403, June 2008.
[34] Menter, F. R., "Review of the Shear-Stress Transport Turbulence Model Experience from an Industrial Perspective," *International Journal of Computational Fluid Dynamics*, Vol. 23, No. 4, 2009, pp. 305–316.
doi:10.1080/10618560902773387
[35] Hopkins, E. J., and Inouye, M., "An Evaluation of Theories for Predicting Turbulent Skin Friction and Heat Transfer on Flat Plates at Supersonic and Hypersonic Mach Numbers," *AIAA Journal*, Vol. 9, No. 6, 1971, pp. 993–1003.
doi:10.2514/3.6323
[36] Baldwin, B. S., and Lomax, H., "Thin-Layer Approximation and Algebraic Model for Separated Turbulent Flows," AIAA Paper 78-257, June 1978.
[37] Dilley, A. D., "Evaluation of CFD Turbulent Heating Prediction Techniques and Comparison with Hypersonic Experimental Data," NASA CR-2001-210837, March 2001.
[38] Cebeci, T., and Smith, A. M. O., *Analysis of Turbulent Boundary Layers*, Academic Press, New York, 1974.
[39] Spalding, D. B., and Chi, S. W., "The Drag of a Compressible Turbulent Boundary Layer on a Smooth Flat Plate with and Without Heat Transfer," *Journal of Fluid Mechanics*, Vol. 18, No. 1, 1964, pp. 117–143.
doi:10.1017/S0022112064000088
[40] White, F. M., *Viscous Fluid Flow*, McGraw–Hill, New York, 1974.
[41] Peterson, J. B., Jr., "A Comparison of Experimental and Theoretical Results for the Compressible Turbulent-Boundary-Layer Skin Friction with Zero Pressure Gradient," NASA TN-D-1795, March 1963.
[42] Roy, C. J., and Blottner, F. G., "Review and Assessment of Turbulence Models for Hypersonic Flows," *Progress in Aerospace Sciences*, Vol. 42, 2006, pp. 469–530.
doi:10.1016/j.paerosci.2006.12.002
[43] van Driest, E. R., "Problem of Aerodynamic Heating," *Aeronautical Engineering Review*, Vol. 15, Oct. 1956, pp. 26–41.
[44] White, F. M., and Christoph, G. H., "Simple Theory for 2-Dimensional Compressible Turbulent Boundary Layer," *Journal of Basic Engineering*, Vol. 94, No. 3, 1972, pp. 636–642.
[45] Spalding, D. B., and Chi, S. W., "Skin Friction Exerted by a Compressible Fluid Stream on a Flat Plate," *AIAA Journal*, Vol. 1, No. 9, 1963, pp. 2160–2161.
doi:10.2514/3.2018
[46] Huang, P. G., Bradshaw, P., and Coakley, T. J., "Skin Friction and Velocity Profile Family for Compressible Turbulent Boundary Layers," *AIAA Journal*, Vol. 31, No. 9, 1993, pp. 1600–1604.
doi:10.2514/3.11820

T. Lin
Associate Editor